



Research paper

Synthesis and characterization of a series of transition metal compounds of thioether and disulfide ligands

Feng Jiang^a, Maxime A. Siegler^b, Elisabeth Bouwman^{a,*}^a Leiden Institute of Chemistry, Gorlaeus Laboratories, Leiden University, P.O. Box 9502, 2300 RA Leiden, the Netherlands^b Department of Chemistry, Johns Hopkins University, 3400 N. Charles Street, Baltimore, MD 21218, United States

ARTICLE INFO

Keywords:

Disulfide ligand
Thioether ligand
Mononuclear compounds
Dinuclear compounds

ABSTRACT

A series of mononuclear metal compounds $[M^II(L^1SCH_3)Cl_2]$ ($M = Co, Cu, Fe, Mn$, $L^1SCH_3 = 2$ -(methylthio)-N,N-bis(pyridin-2-ylmethyl)aminoethane) has been synthesized and characterized. The structures and spectroscopic properties of these compounds are compared to the related dinuclear compounds $[M_2^II(L^1SSL^1)Cl_4]$ ($M = Co, Cu, Fe$), which were obtained from the reactions of disulfide ligand L^1SSL^1 with the corresponding metal chloride salts ($L^1SSL^1 = di$ -2-(bis(2-pyridylmethyl)amino)-ethyl disulfide). The crystal structures show that the metal centers in the mononuclear compounds $[Co^II(L^1SCH_3)Cl_2]$, $[Cu^II(L^1SCH_3)Cl_2]$ and $[Mn^II(L^1SCH_3)Cl_2]$ are in trigonal-bipyramidal geometries coordinated by three nitrogen donors of the tetradentate ligand and two chloride ions, with configurations similar to that of metal centers in $[Co_2^II(L^1SSL^1)Cl_4]$ and $[Cu_2^II(L^1SSL^1)Cl_4]$. In contrast, the iron(II) center in $[Fe^II(L^1SCH_3)Cl_2]$ is coordinated by three nitrogen donors and one sulfur atom of the tetradentate ligand and two chloride ions in an octahedral geometry, which is similar to the geometry of one of the Fe(II) centers in the dinuclear compound $[Fe_2^II(L^1SSL^1)Cl_4]$, where two iron (II) centers are in different geometries. UV–vis spectra of the mononuclear compounds are comparable to those of the related dinuclear compounds.

1. Introduction

The synthesis of transition metal compounds to mimic active sites in sulfur-rich metalloenzymes has received considerable attention in the last decades, as it provides a uniquely chemical perspective into the functions of metalloenzymes in e.g. oxidation, electron transfer, and nitrogen fixation [1–5]. Metal compounds with sulfur donors can be synthesized from disulfide, thioether or thiolate-containing ligands. Generally, the sulfur atoms in disulfide and thioether groups are rather weak donor atoms, quite often not coordinating to the metal center. On the other hand, thiolate ligands are highly oxidation sensitive, resulting in the formation of disulfides or oxygenated sulfur donors. In the past few years, however, the use of disulfide ligands has been shown to result in the formation of either low-valent metal disulfide compounds or high-valent metal thiolate compounds. This intriguing redox interconversion has been investigated mainly for copper, but more recently also for cobalt (Scheme 1) [6–11]. Such studies assist in gaining understanding of the disulfide-thiolate conversion and electron transfer in metalloenzymes, such as the Cu_A site of cytochrome *c* oxidase. Thiolate ligands are frequently used to synthesize especially iron and nickel compounds [12–14]. Their reactivity

with oxidizing agents is further explored to elaborate on the mechanism of degradation of metalloenzymes such as cysteine dioxygenase (CDO) by dioxygen [15–19]. Metal compounds containing thioether ligands are studied as mimics for the active site in enzymes such as galactose oxidase [20,21].

In the last few years, our group synthesized metal disulfide compounds $[M_2^II(L^1SSL^1)Cl_4]$ ($M = Co, Fe$) from the disulfide ligand L^1SSL^1 ($L^1SSL^1 = di$ -2-(bis(2-pyridylmethyl)amino)-ethyl disulfide, see Scheme 1) in reactions with the metal(II) chloride salts [22]. The two iron(II) centers in $[Fe_2^II(L^1SSL^1)Cl_4]$ are in different geometries: one is coordinated by three nitrogen donors and one sulfur atom of the ligand, and two chloride ions in an octahedral geometry, whereas the other is coordinated by three nitrogen donors of the ligand and two chloride ions in a trigonal-bipyramidal geometry [22]. Herein we report the synthesis of a series of metal compounds (Fe, Co, Cu, Mn) of the thioether-containing ligand L^1SCH_3 ($L^1SCH_3 = 2$ -(methylthio)-N,N-bis(pyridin-2-ylmethyl)aminoethane). The spectroscopic and structural properties of these compounds have been investigated and are compared with those of the related dinuclear metal disulfide compounds.

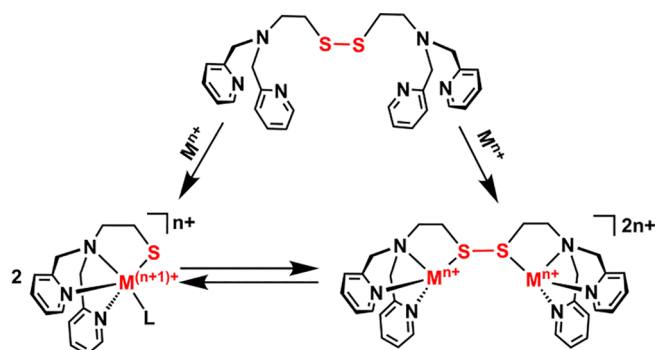
* Corresponding author.

E-mail address: bouwman@lic.leidenuniv.nl (E. Bouwman).<https://doi.org/10.1016/j.ica.2018.10.047>

Received 16 August 2018; Received in revised form 22 October 2018; Accepted 23 October 2018

Available online 24 October 2018

0020-1693/ © 2018 The Authors. Published by Elsevier B.V. This is an open access article under the CC BY-NC-ND license (<http://creativecommons.org/licenses/by-nc-nd/4.0/>).



Scheme 1. Synthesis of low-valent metal disulfide compounds and high-valent metal thiolate compounds from disulfide ligands ($M = \text{Cu}$, or Co ; $n = 1$ for Cu and $n = 2$ for Co).

2. Experimental

2.1. General procedures

All chemicals were purchased from commercial vendors and used as received unless noted otherwise. Acetonitrile and diethyl ether were obtained from a solvent purification system (PureSolv 400). Methanol, acetone and hexane were acquired from commercial sources and stored on 3 Å molecular sieves. The synthesis of Co(II) , Cu(II) and Mn(II) compounds was carried out in air, whereas the synthesis of Fe(II) compounds was carried out under an inert atmosphere using standard Schlenk-line techniques. ^1H NMR and ^{13}C NMR spectra of the ligands L^1SSL^1 and L^1SCH_3 were recorded on a Bruker 300 DPX spectrometer. Mass spectra were recorded on a Finnigan Aqua mass spectrometer with electrospray ionization (ESI). IR spectra were acquired on a PerkinElmer UATR spectrum equipped with single reflection diamond (scan range $400\text{--}4000\text{ cm}^{-1}$, resolution 4 cm^{-1}). UV–vis spectra were collected using a transmission dip probe with variable path length and reflection probe on an Avantes Avaspec-2048 spectrometer with Avalight-DH-S-BAL light source. Effective magnetic moments of the compounds were measured in solution by the Evans method, and in the solid state using a magnetic susceptibility balance (Johnson Matthey). Elemental analyses were performed by the Microanalytical Laboratory Kolbe in Germany.

2.2. Single crystal X-ray crystallography

All reflection intensities were measured at 110(2) K using a SuperNova diffractometer (equipped with Atlas detector) with $\text{Mo K}\alpha$ radiation ($\lambda = 0.71073\text{ \AA}$) for compounds $[\text{Co}^{\text{II}}(\text{L}^1\text{SCH}_3)_2\text{Cl}_2]$, $[\text{Cu}^{\text{II}}(\text{L}^1\text{SCH}_3)_2\text{Cl}_2]$, $[\text{Mn}^{\text{II}}(\text{L}^1\text{SCH}_3)_2\text{Cl}_2]$, and $[\text{Fe}^{\text{II}}(\text{L}^1\text{SCH}_3)_2\text{Cl}_2]$, and with $\text{Cu K}\alpha$ radiation ($\lambda = 1.54178\text{ \AA}$) for the compound $[\text{Cu}_2^{\text{II}}(\text{L}^1\text{SSL}^1)_4\text{Cl}_4]$ under the program CrysAlisPro (Version CrysAlisPro 1.171.39.29c, Rigaku OD, 2017 or Version 1.171.36.32 Agilent Technologies, 2013). The same program was used to refine the cell dimensions and for data reduction. The structure was solved with the program SHELXS-2014/7 [23], and was refined on F^2 with SHELXL-2014/7. Numerical absorption correction based on Gaussian integration over a multifaceted crystal model was applied using CrysAlisPro for $[\text{Co}^{\text{II}}(\text{L}^1\text{SCH}_3)_2\text{Cl}_2]$, $[\text{Cu}^{\text{II}}(\text{L}^1\text{SCH}_3)_2\text{Cl}_2]$, $[\text{Mn}^{\text{II}}(\text{L}^1\text{SCH}_3)_2\text{Cl}_2]$, and $[\text{Fe}^{\text{II}}(\text{L}^1\text{SCH}_3)_2\text{Cl}_2]$. Analytical numeric absorption correction using a multifaceted crystal model was applied using CrysAlisPro for $[\text{Cu}_2^{\text{II}}(\text{L}^1\text{SSL}^1)_4\text{Cl}_4]$. The temperature of the data collection was controlled using the system Cryojet (manufactured by Oxford Instruments). The H atoms were placed at calculated positions using the instructions AFIX 23, AFIX 43 or AFIX 137 with isotropic displacement parameters having values 1.2 or 1.5 Ueq of the attached C atoms.

The structure of $[\text{Co}^{\text{II}}(\text{L}^1\text{SCH}_3)_2\text{Cl}_2]$ is ordered. The absolute structure configuration was established by anomalous-dispersion effects in diffraction measurements on the crystal, and the Flack and Hoof

parameters refine to 0.011(5) and 0.013(3), respectively. The structures of $[\text{Cu}^{\text{II}}(\text{L}^1\text{SCH}_3)_2\text{Cl}_2]$, $[\text{Fe}^{\text{II}}(\text{L}^1\text{SCH}_3)_2\text{Cl}_2]$, $[\text{Mn}^{\text{II}}(\text{L}^1\text{SCH}_3)_2\text{Cl}_2]$ are ordered. The structure of $[\text{Cu}_2^{\text{II}}(\text{L}^1\text{SSL}^1)_4\text{Cl}_4]$ is partly disordered. The asymmetric unit contains two crystallographically independent molecules. The C1X-C2X-S1X fragments ($X = \text{A}, \text{B}$) are disordered over two orientations, and the occupancy factors of the major components of the disorder refine to 0.798(13) and 0.673(11). The crystal is pseudomerohedrally twinned, and the twin relationship is given by $M = (-1\ 0\ 0 / 0\ -1\ 0\ 0 / 0\ 0\ 1)$. The general and racemic twinning were refined simultaneously using the instruction TWIN $-1\ 0\ 0\ 0\ -1\ 0\ 0\ 0\ 1\ -4$, and the three BASF twin component factors refine to 0.230(13), 0.226(15) and 0.215(13).

2.3. Synthesis of compounds

$[\text{Co}^{\text{II}}(\text{L}^1\text{SCH}_3)_2\text{Cl}_2]$

The ligand L^1SCH_3 (54.7 mg, 0.2 mmol) was dissolved in 2 mL acetonitrile, and separately $\text{CoCl}_2\cdot 6\text{H}_2\text{O}$ (47.8 mg, 0.2 mmol) was dissolved in 2 mL acetonitrile. The two solutions were mixed resulting in a purple suspension, which was stirred for another 30 min. Then, 20 mL diethyl ether was added and a purple precipitate was formed immediately. The obtained precipitate was washed with diethyl ether ($3 \times 20\text{ mL}$). Yield: 45.1 mg, 0.1 mmol, 56%. After two days single crystals suitable for X-ray structure determination were obtained upon slow vapor diffusion of diethyl ether into an acetonitrile solution of the compound at room temperature. IR (cm^{-1}): 487m, 507m, 646m, 763s, 787s, 1022s, 1053m, 1097m, 1154m, 1308m, 1440s, 1479m, 1605s. ESI-MS found (calcd) for $[\text{M}-\text{Cl}]^+$ m/z : 367.2 (367.1). Elemental analysis calcd (%) for $\text{C}_{15}\text{H}_{19}\text{Cl}_2\text{CoN}_3\text{S}$: C 44.68, H 4.75, N 10.42; Found: C 44.02, H 4.89, N 10.27.

$[\text{Fe}^{\text{II}}(\text{L}^1\text{SCH}_3)_2\text{Cl}_2]$

To a yellow solution of L^1SCH_3 (48.6 mg, 0.2 mmol) dissolved in 5 mL methanol, solid $\text{FeCl}_2\cdot 4\text{H}_2\text{O}$ (35.4 mg, 0.2 mmol) was added, immediately resulting in a yellow solution. The obtained solution was stirred for 2 h at room temperature under inert atmosphere. After that, 50 mL diethyl ether was added, yielding a yellow precipitate. The obtained precipitate was washed with diethyl ether ($3 \times 20\text{ mL}$). Yield: 32 mg, 0.1 mmol, 45%. After around 1 week single crystals suitable for X-ray structure determination were obtained upon slow vapor diffusion of diethyl ether into a methanolic solution of the compound at room temperature. IR (cm^{-1}): 481w, 640w, 729w, 776m, 794s, 983w, 1017m, 1050m, 1294m, 1442m, 1475m, 1601m. ESI-MS found (calcd) for $[\text{M}-\text{Cl}]^+$ m/z : 364.5 (364.7). Elemental analysis calcd (%) for $\text{C}_{15}\text{H}_{19}\text{Cl}_2\text{FeN}_3\text{S} + \text{H}_2\text{O}$: C 43.08, H 5.06, N 10.05; Found: C 42.64, H 4.65, N 10.34.

$[\text{Cu}^{\text{II}}(\text{L}^1\text{SCH}_3)_2\text{Cl}_2]$

Ligand L^1SCH_3 (160.3 mg, 0.6 mmol) was dissolved in 10 mL acetonitrile. To this solution solid CuCl_2 (78.9 mg, 0.6 mmol) was added, yielding a blue solution. The obtained solution was stirred overnight at room temperature, after which 80 mL diethyl ether was added, resulting in a blue precipitate. The solid was collected by filtration and was washed with diethyl ether ($4 \times 5\text{ mL}$). Yield: 172.1 mg, 0.4 mmol, 72%. After around one week single crystals suitable for X-ray structure determination were obtained upon vapor diffusion of diethyl ether into an acetonitrile solution of the compound at room temperature. IR (cm^{-1}): 1606s, 1573w, 1479s, 1442s, 1379w, 1351w, 1310w, 1286w, 1153m, 1111m, 1094s, 1052s, 1027s, 992m, 962w, 852m, 787s, 771s, 727m, 652m, 536m. ESI-MS found (calcd) for $[\text{M}-\text{Cl}]^+$ m/z : 371.0 (371.0). Elemental analysis calcd (%) for $\text{C}_{15}\text{H}_{19}\text{Cl}_2\text{CuN}_3\text{S} + 0.3\text{ C}_4\text{H}_{10}\text{O}$: C 45.24, H 5.16, N 9.77; Found: C 44.64, H 5.25, N 9.61.

$[\text{Mn}^{\text{II}}(\text{L}^1\text{SCH}_3)_2\text{Cl}_2]$

Ligand L^1SCH_3 (206.4 mg, 0.8 mmol) was dissolved in 10 mL methanol. To this solution solid $\text{MnCl}_2\cdot 4\text{H}_2\text{O}$ (149.5 mg, 0.8 mmol) was

added, yielding a pale yellow solution. The obtained solution was stirred for overnight at room temperature. Then, 80 mL diethyl ether was added, leading to a pale-yellow, oily material. The solution was decanted and the obtained oily material was re-dissolved in 10 mL acetonitrile. To the resulting solution 80 mL diethyl ether was added, yielding a pale yellow precipitate, which was collected by filtration and washed with diethyl ether (4×5 mL). Yield: 177 mg, 0.4 mmol, 58%. After around one week single crystals suitable for X-ray structure determination were obtained upon slow vapor diffusion of diethyl ether into an acetonitrile solution of the compound at room temperature. IR (cm^{-1}): 1602s, 1569m, 1477m, 1443s, 1295s, 1161m, 1094m, 1050m, 1016s, 794s, 775s, 730m, 641m. ESI-MS found (calcd) for $[\text{M}-\text{Cl}]^+$ m/z 363.0 (363.0). Elemental analysis calcd (%) for $\text{C}_{15}\text{H}_{19}\text{Cl}_2\text{MnN}_3\text{S} + 0.5 \text{H}_2\text{O}$: C 44.13, H 4.94, N 10.29; Found: C 43.84, H 4.90, N 10.19.

$[\text{Cu}_2^{\text{II}}(\text{L}^1\text{SSL}^1)\text{Cl}_4]$

To a solution of L^1SSL^1 (103.3 mg, 0.2 mmol) in 4 mL acetonitrile, solid CuCl_2 (53.8 mg, 0.4 mmol) was added, resulting in a blue solution. The obtained solution was stirred for about 30 min, during which time a blue precipitate formed. The blue precipitate was collected by filtration and washed with diethyl ether (3×10 mL). Yield: 70.7 mg, 0.1 mmol, 45%. After approximately one month single crystals suitable for X-ray structure determination were obtained by slow evaporation of a solution of the compound in dimethylformamide in the back of a fume hood at room temperature. IR (cm^{-1}): 1607s, 1572w, 1479m, 1441s, 1350w, 1305w, 1286m, 1249w, 1103w, 1053s, 1029s, 963w, 978w, 877m, 819w, 784vs, 762vs, 723w, 652w. ESI-MS found (calcd) for $\frac{1}{2}[\text{M}-2\text{Cl}]^{2+}$ m/z 357.1 (357.3); $[\text{M}-\text{Cl}]^+$ m/z 749.0 (749.0). Elemental analysis calcd (%) for $\text{C}_{28}\text{H}_{32}\text{Cl}_4\text{Cu}_2\text{N}_6\text{S}_2 + 0.5 \text{H}_2\text{O}$: C 42.32, H 4.19, N 10.58; Found: C 42.43, H 4.21, N 10.59.

3. Results

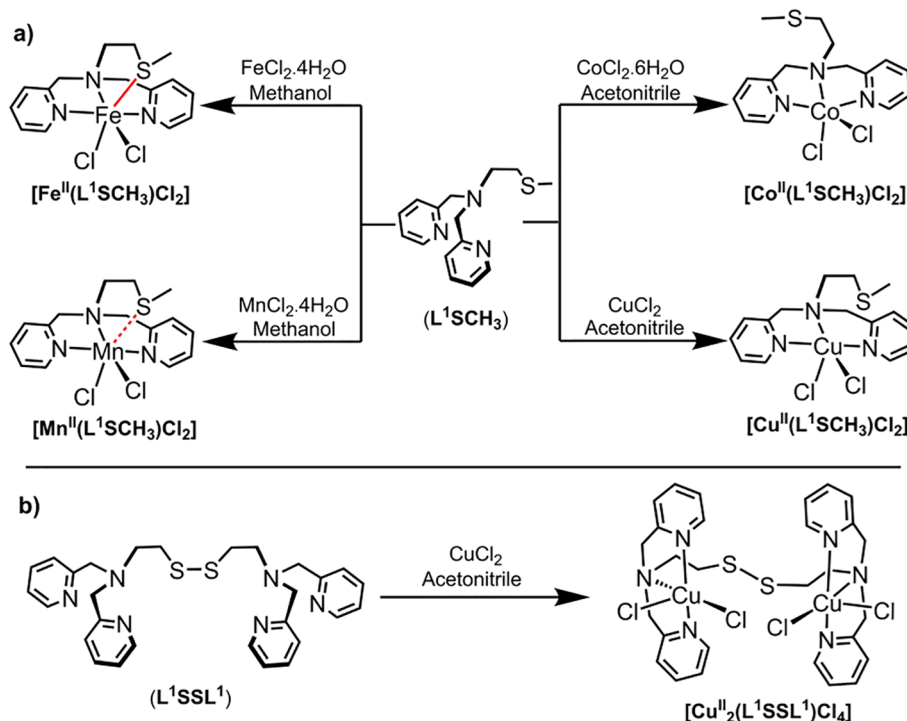
The ligands L^1SSL^1 and L^1SCH_3 (Scheme 2) were synthesized via reported procedures [10,21]. The reactions with cobalt(II), manganese(II) and copper(II) chloride salts ($\text{CoCl}_2 \cdot 6\text{H}_2\text{O}$, CuCl_2 , $\text{MnCl}_2 \cdot 4\text{H}_2\text{O}$) were

carried out in air, whereas reactions with $\text{FeCl}_2 \cdot 4\text{H}_2\text{O}$ were performed under oxygen-free conditions. The addition of one equivalent of the metal (II) chlorides to one equivalent of thioether ligand L^1SCH_3 dissolved in acetonitrile or methanol led to the formation of compounds $[\text{Co}^{\text{II}}(\text{L}^1\text{SCH}_3)\text{Cl}_2]$ (yield 56%), $[\text{Mn}^{\text{II}}(\text{L}^1\text{SCH}_3)\text{Cl}_2]$ (yield 58%), $[\text{Cu}^{\text{II}}(\text{L}^1\text{SCH}_3)\text{Cl}_2]$ (yield 72%), and $[\text{Fe}^{\text{II}}(\text{L}^1\text{SCH}_3)\text{Cl}_2]$ (yield 45%). Reaction of two equivalents of CuCl_2 with one equivalent of the disulfide ligand L^1SSL^1 dissolved in acetonitrile led to the formation of the dinuclear compound $[\text{Cu}_2^{\text{II}}(\text{L}^1\text{SSL}^1)\text{Cl}_4]$ in a yield of 45%. All compounds were further characterized with ESI-MS spectrometry, IR and UV-vis spectroscopy, single crystal X-ray crystallography, and elemental analysis.

Single crystals of $[\text{Co}^{\text{II}}(\text{L}^1\text{SCH}_3)\text{Cl}_2]$, $[\text{Fe}^{\text{II}}(\text{L}^1\text{SCH}_3)\text{Cl}_2]$, $[\text{Cu}^{\text{II}}(\text{L}^1\text{SCH}_3)\text{Cl}_2]$, and $[\text{Mn}^{\text{II}}(\text{L}^1\text{SCH}_3)\text{Cl}_2]$ suitable for X-ray structure determination were obtained by slow vapor diffusion of diethyl ether into solutions of the compounds. Single crystals of $[\text{Cu}_2^{\text{II}}(\text{L}^1\text{SSL}^1)\text{Cl}_4]$ were obtained by slow evaporation of a DMF solution of the compound. Crystallographic and refinement data for each structure are collected in the Supporting Information, Tables S1 and S2. Projections of the structures are shown in Figs. 1 and 2; selected bond distances and angles are given in Tables 1 and 2. Stacking interactions are not present in any of the structures, despite the presence of the pyridine rings.

The compound $[\text{Co}^{\text{II}}(\text{L}^1\text{SCH}_3)\text{Cl}_2]$ crystallizes in the monoclinic space group Cc with one mononuclear compound in the asymmetric unit. The Co(II) ion is coordinated by three nitrogen donors of the tetradentate ligand and two chloride ions in a distorted trigonal-bipyramidal geometry with a τ value of 0.77 [24]. The Co–N bond lengths range from 2.074(2) to 2.2990(19) Å, whereas the two Co–Cl bond lengths are very similar (2.3046(6) and 2.3049(6) Å).

The compounds $[\text{Fe}^{\text{II}}(\text{L}^1\text{SCH}_3)\text{Cl}_2]$, $[\text{Mn}^{\text{II}}(\text{L}^1\text{SCH}_3)\text{Cl}_2]$, and $[\text{Cu}^{\text{II}}(\text{L}^1\text{SCH}_3)\text{Cl}_2]$ all crystallize in the monoclinic space group $P2_1/c$ with one complex molecule in the asymmetric unit. In all three compounds the three nitrogen donor atoms of the ligand are bound to the metal center in a meridional arrangement, and both chloride anions are coordinated. The compounds differ in their interactions with the sulfur donor atom of the tetradentate ligand. The Fe(II) center is in a slightly distorted octahedral geometry completed by coordination of the sulfur atom of the tetradentate ligand. The Fe1–S1 bond distance is



Scheme 2. Schematic overview of the reactions of the ligands L^1SCH_3 and L^1SSL^1 with metal chloride salts.

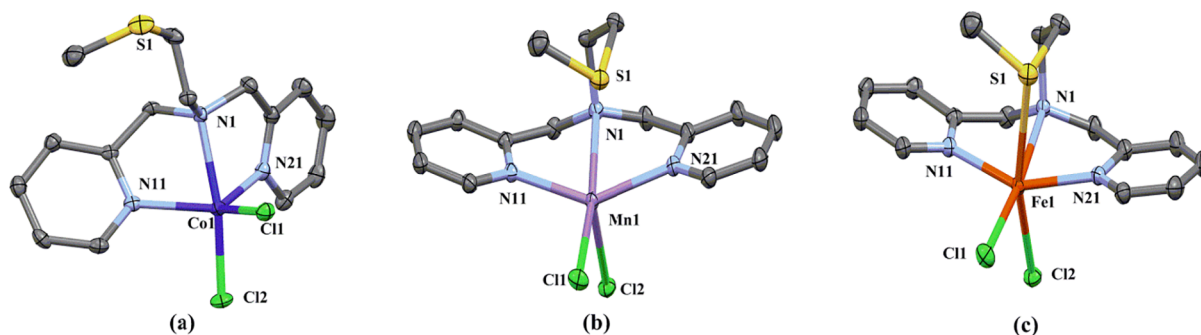


Fig. 1. Displacement ellipsoid plots (50% probability level) of compounds (a) $[\text{Co}^{\text{II}}(\text{L}^1\text{SCH}_3)\text{Cl}_2]$, (b) $[\text{Mn}^{\text{II}}(\text{L}^1\text{SCH}_3)\text{Cl}_2]$; (c) $[\text{Fe}^{\text{II}}(\text{L}^1\text{SCH}_3)\text{Cl}_2]$ at 110(2) K. All hydrogen atoms are omitted for clarity.

2.6972(6) Å, and the Fe–N bond lengths range between 2.1689(16) and 2.2773(15) Å. The Fe–Cl2 bond length of 2.4481(5) Å is slightly longer than Fe1–Cl1 bond length (2.3275(5) Å), indicative of the larger *trans* influence of the thioether donor.

The coordination sphere of the Mn(II) ion is in between square pyramidal and trigonal bipyramidal with a τ value of 0.42. The Mn–S bond distance is 2.8325(4) Å, indicating a weak electrostatic interaction most likely causing the change in geometry to square pyramidal, as compared to the cobalt compound. However, this Mn–S distance is significantly longer than that found in $[\text{Fe}^{\text{II}}(\text{L}^1\text{SCH}_3)\text{Cl}_2]$. The Mn–N bond lengths range between 2.2366(10) and 2.3503(10) Å, and thus are slightly longer than the Co–N bond lengths in $[\text{Co}^{\text{II}}(\text{L}^1\text{SCH}_3)\text{Cl}_2]$.

The Cu(II) ion is in a distorted square-pyramidal geometry with a τ value of 0.22. The Cu–S distance is 2.9961(4) Å, which is again longer than the Mn–S distance in $[\text{Mn}^{\text{II}}(\text{L}^1\text{SCH}_3)\text{Cl}_2]$. The Cu–N bond lengths are in the range of 2.0061(11)–2.0789(11) Å, much shorter than those in the other compounds. Cl2 is located in the axial position with a bond distance of 2.6570(4) Å, whereas the Cu–Cl1 bond length in the basal plane is 2.2673(3) Å.

The compound $[\text{Cu}_2^{\text{II}}(\text{L}^1\text{SSL}^1)\text{Cl}_4]$ crystallizes in the monoclinic space group $P2_1$, with two crystallographically independent molecules in the asymmetric unit. As the two independent molecules have similar conformations, the description is based on one molecule only (molecule A with Cu1/Cu2). Both Cu(II) centers in $[\text{Cu}_2^{\text{II}}(\text{L}^1\text{SSL}^1)\text{Cl}_4]$ are coordinated by two chloride ions, and three nitrogen atoms of the ligand. However, the τ value for Cu1 (0.03, square pyramidal geometry) significantly differs from that for Cu2 (0.33, distorted square pyramidal geometry). The Cu–N bond lengths range between 2.005(5) and 2.101(8) Å, similar as in $[\text{Cu}^{\text{II}}(\text{L}^1\text{SCH}_3)\text{Cl}_2]$, but shorter than in $[\text{Co}_2^{\text{II}}(\text{L}^1\text{SSL}^1)\text{Cl}_4]$ [22]. The sulfur atoms of the disulfide bond are non-coordinating. The distances between Cu1–S1 and Cu2–S2 are 3.113(4) and 4.824(2) Å, respectively, which are much longer than that in $[\text{Cu}^{\text{II}}(\text{L}^1\text{SCH}_3)\text{Cl}_2]$. The shorter Cu1–S1 distance may be the cause of

the difference in coordination geometry of the two copper ions.

UV–vis spectra of $[\text{Co}^{\text{II}}(\text{L}^1\text{SCH}_3)\text{Cl}_2]$ dissolved in acetonitrile present three absorption bands. The absorption band at 256 nm ($\epsilon = 4.1 \times 10^3 \text{ M}^{-1} \text{ cm}^{-1}$) is assigned to the $\pi^* \leftarrow \pi$ transition of the pyridyl groups, whereas the two bands at 548 ($\epsilon = 2.0 \times 10^2 \text{ M}^{-1} \text{ cm}^{-1}$) and 629 ($\epsilon = 1.5 \times 10^2 \text{ M}^{-1} \text{ cm}^{-1}$) nm arise from *d-d* transitions of the cobalt(II) ion, likely combined with a $\text{Co}^{\text{II}} \leftarrow \text{Cl}$ charge transfer transition (LMCT) (Fig. 3a, red line) [25]. ESI-MS spectra of this compound dissolved in acetonitrile show a dominant peak (m/z) at 367.2 corresponding to the fragment $[\text{Co}^{\text{II}}(\text{L}^1\text{SCH}_3)\text{Cl}]^+$ (Fig. S1). The effective magnetic moment of $[\text{Co}^{\text{II}}(\text{L}^1\text{SCH}_3)\text{Cl}_2]$ was determined, showing a μ_{eff} of 4.12 μ_{B} in the solid state, and 4.52 μ_{B} in dmsol solution [26,27]. Both values are consistent with a high-spin ($S = 3/2$) Co(II) center (3.87 is expected for $S = 3/2$). The absorption spectrum of the compound in the solid state apart from the intense charge transfer band at 257 nm, shows three *d-d* transitions at 549, 653, and 876 nm typical for a 5-coordinate cobalt(II) ion (Fig. S2) [28].

UV–vis spectra of $[\text{Fe}^{\text{II}}(\text{L}^1\text{SCH}_3)\text{Cl}_2]$ dissolved in methanol reveal two absorption bands and a shoulder (Fig. 3a, black line). The absorption band at 254 nm ($\epsilon = 4.0 \times 10^3 \text{ M}^{-1} \text{ cm}^{-1}$) is ascribed to the $\pi^* \leftarrow \pi$ transition of pyridyl groups, whereas the band at 396 ($\epsilon = 1.0 \times 10^3 \text{ M}^{-1} \text{ cm}^{-1}$) nm is tentatively assigned to a metal-to-ligand charge transfer transition (MLCT). The UV–vis spectrum is similar to that of the related dinuclear compound $[\text{Fe}_2^{\text{II}}(\text{L}^1\text{SSL}^1)\text{Cl}_4]$ [22]. The ESI-MS spectrum of the compound dissolved in methanol presents a dominant peak (m/z) at 364.5 for the cationic species $[\text{Fe}^{\text{II}}(\text{L}^1\text{SCH}_3)\text{Cl}]^+$ in addition to a peak of the solvated species $[\text{Fe}^{\text{II}}(\text{L}^1\text{SCH}_3)\text{Cl}(\text{MeOH})]^+$ ($m/z = 395.5$; Fig. S3). The effective magnetic moment of $[\text{Fe}^{\text{II}}(\text{L}^1\text{SCH}_3)\text{Cl}_2]$ dissolved in methanol was estimated using the Evans' method, giving a μ_{eff} of 4.61 μ_{B} . This value is in agreement with a high-spin Fe(II) center (4.90 is expected for $S = 2$). The absorption spectrum of the compound in the solid state shows a

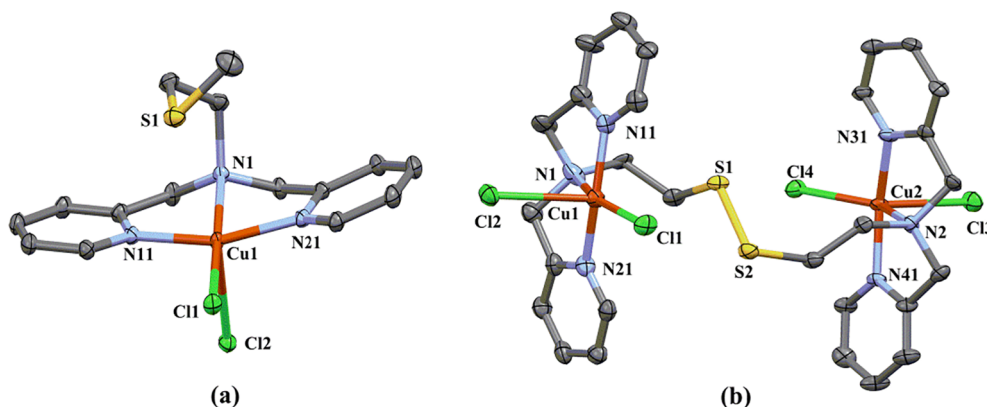


Fig. 2. Displacement ellipsoid plots (50% probability level) of compounds (a) $[\text{Cu}^{\text{II}}(\text{L}^1\text{SCH}_3)\text{Cl}_2]$, (b) $[\text{Cu}_2^{\text{II}}(\text{L}^1\text{SSL}^1)\text{Cl}_4]$ at 110(2) K. All hydrogen atoms are omitted for clarity.

Table 1Selected bond distances and angles of compounds $[\text{Co}^{\text{II}}(\text{L}^1\text{SCH}_3)_2\text{Cl}_2]$, $[\text{Cu}^{\text{II}}(\text{L}^1\text{SCH}_3)_2\text{Cl}_2]$, $[\text{Mn}^{\text{II}}(\text{L}^1\text{SCH}_3)_2\text{Cl}_2]$ and $[\text{Fe}^{\text{II}}(\text{L}^1\text{SCH}_3)_2\text{Cl}_2]$.

Distances/Angles	$[\text{Co}^{\text{II}}(\text{L}^1\text{SCH}_3)_2\text{Cl}_2]$	$[\text{Cu}^{\text{II}}(\text{L}^1\text{SCH}_3)_2\text{Cl}_2]$	$[\text{Mn}^{\text{II}}(\text{L}^1\text{SCH}_3)_2\text{Cl}_2]$	$[\text{Fe}^{\text{II}}(\text{L}^1\text{SCH}_3)_2\text{Cl}_2]$
M1-N1	2.2990(19)	2.0789(11)	2.3503(10)	2.2773(15)
M1-N11	2.074(2)	2.0069(11)	2.2366(10)	2.1689(16)
M1-N21	2.083(2)	2.0061(11)	2.2550(10)	2.1781(16)
M1-S1	5.8887(8)	2.9961(4)	2.8325(4)	2.6972(6)
M1-Cl1	2.3049(6)	2.2673(3)	2.3858(4)	2.3275(5)
M1-Cl2	2.3046(6)	2.6570(4)	2.4513(4)	2.4481(5)
N11-M1-N21	119.35(7)	161.05(5)	144.54(4)	148.85(6)
N11-M1-N1	75.89(7)	81.20(4)	72.85(4)	74.70(6)
N21-M1-N1	75.92(7)	81.05(4)	73.12(4)	75.03(6)
N11-M1-Cl2	95.29(6)	89.80(3)	98.27(3)	96.38(4)
N21-M1-Cl2	99.59(6)	96.62(3)	91.22(3)	90.33(4)
N1-M1-Cl2	165.81(5)	89.45(3)	89.68(3)	89.08(4)
N11-M1-Cl1	119.06(6)	99.30(3)	101.36(3)	100.72(4)
N21-M1-Cl1	114.38(6)	97.67(3)	110.69(3)	108.66(4)
N1-M1-Cl1	91.79(5)	174.05(3)	169.90(3)	172.98(4)
Cl2-M1-Cl1	102.27(2)	96.473(12)	99.468(13)	96.795(19)
N11-M1-S1	–	74.45(3)	90.00(3)	92.10(4)
N21-M1-S1	–	96.10(3)	72.84(3)	75.45(4)
N1-M1-S1	–	80.59(3)	76.92(3)	79.82(4)
Cl1-M1-S1	–	93.807(12)	95.049(12)	95.184(18)
Cl2-M1-S1	–	162.414(12)	161.494(12)	163.767(19)

Table 2Selected bond distances and angles of compound $[\text{Cu}_2^{\text{II}}(\text{L}^1\text{SSL}^1)\text{Cl}_4]$ (only values for molecule A with the Cu1 and Cu2 metal centers are provided).

Distances (Å)	Angles (°)				
Cu1-N1	2.101(8)	N11-Cu1-N21	161.4(3)	N41-Cu2-N31	162.7(2)
Cu1-N11	2.008(7)	N11-Cu1-N1	80.8(3)	N41-Cu2-N2	81.5(2)
Cu1-N21	2.010(7)	N21-Cu1-N1	81.1(3)	N31-Cu2-N2	81.3(3)
Cu1-Cl1	2.266(2)	N11-Cu1-Cl1	98.48(18)	N41-Cu2-Cl4	96.24(18)
Cu1-Cl2	2.561(2)	N21-Cu1-Cl1	97.5(2)	N31-Cu2-Cl4	96.30(18)
Cu2-N2	2.071(6)	N1-Cu1-Cl1	163.0(2)	N2-Cu2-Cl4	142.87(18)
Cu2-N31	2.012(6)	N11-Cu1-Cl2	91.78(18)	N41-Cu2-Cl3	90.49(17)
Cu2-N41	2.005(5)	N21-Cu1-Cl2	94.00(19)	N31-Cu2-Cl3	94.17(18)
Cu2-Cl3	2.447(2)	N1-Cu1-Cl2	94.3(2)	N2-Cu2-Cl3	99.53(18)
Cu2-Cl4	2.2628(18)	Cl1-Cu1-Cl2	102.69(8)	Cl4-Cu2-Cl3	117.58(7)
S1-S2	2.032(3)				
Cu1-Cu2	7.762(1)				

broad absorption from 250 to 500 nm for the charge transfer transitions, in addition to a weak *d-d* transition at ~ 1000 nm (Fig. S4).

The UV-vis spectrum of compound $[\text{Mn}^{\text{II}}(\text{L}^1\text{SCH}_3)_2\text{Cl}_2]$ dissolved in acetonitrile presents essentially a single absorption band at 260 nm

($\epsilon = 1.1 \times 10^4 \text{ M}^{-1} \text{ cm}^{-1}$) ascribed to the $\pi^* \leftarrow \pi$ transition of the pyridyl groups. A weak band at 317 nm ($\epsilon = 4 \times 10^2 \text{ M}^{-1} \text{ cm}^{-1}$) is tentatively assigned to a Mn \leftarrow Cl charge-transfer transition (LMCT) (Fig. 3b, red line). The ESI-MS spectrum of the compound dissolved in

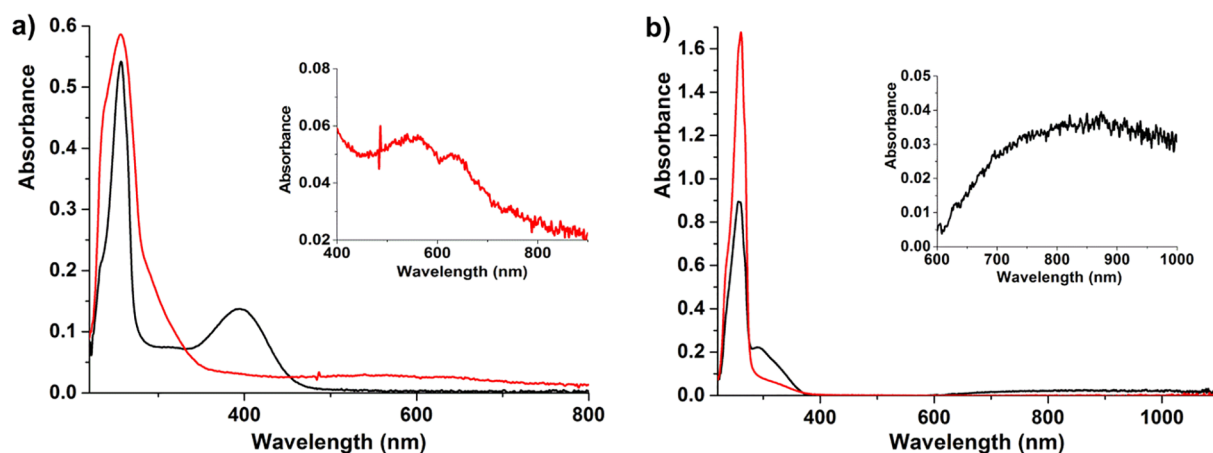


Fig. 3. a) UV-vis spectra of compound $[\text{Co}^{\text{II}}(\text{L}^1\text{SCH}_3)_2\text{Cl}_2]$ dissolved in acetonitrile (red line) and $[\text{Fe}^{\text{II}}(\text{L}^1\text{SCH}_3)_2\text{Cl}_2]$ dissolved in methanol (black line), recorded using solutions 1 mM in [Co] or [Fe] with a transmission dip probe path length of 1.3 mm. The inset shows the UV-vis spectrum recorded using a solution 2 mM in [Co]. b) UV-vis spectra of compounds $[\text{Cu}^{\text{II}}(\text{L}^1\text{SCH}_3)_2\text{Cl}_2]$ (black line) and $[\text{Mn}^{\text{II}}(\text{L}^1\text{SCH}_3)_2\text{Cl}_2]$ (red line) dissolved in acetonitrile, respectively, recorded using a solution 1 mM in [Cu] or [Mn] with a transmission dip probe path length of 1.2 mm. The inset shows the UV-vis spectrum of a solution 2 mM in [Cu]. (For interpretation of the references to colour in this figure legend, the reader is referred to the web version of this article.)

methanol shows a peak (m/z) at 363.0 corresponding to the fragment $[\text{Mn}^{\text{II}}(\text{L}^1\text{SCH}_3)\text{Cl}]^+$ (Fig. S5). The effective magnetic moment of the compound was found to be $6.56 \mu_{\text{B}}$ in acetonitrile solution, and $5.38 \mu_{\text{B}}$ in the solid state, in agreement with a high-spin Mn(II) center ($S = 5/2$). The absorption spectrum of the solid compound only shows the charge-transfer bands (Fig. S6).

The UV-vis spectrum of $[\text{Cu}^{\text{II}}(\text{L}^1\text{SCH}_3)\text{Cl}_2]$ dissolved in methanol presents three absorption bands. The absorption band at 256 nm ($\epsilon = 7.4 \times 10^3 \text{ M}^{-1} \text{ cm}^{-1}$) is assigned to the $\pi^* \leftarrow \pi$ transition of the pyridyl groups, whereas the band at 290 nm ($\epsilon = 1.8 \times 10^3 \text{ M}^{-1} \text{ cm}^{-1}$) probably arises from a $\text{Cu} \leftarrow \text{Cl}$ charge transfer transition (LMCT) (Fig. 3b, black line). A weak band at 814 nm ($2 \times 10^2 \text{ M}^{-1} \text{ cm}^{-1}$) corresponds to the $d-d$ transition of the Cu(II) center. The ESI-MS spectrum of the compound dissolved in acetonitrile shows a dominant peak (m/z) at 371.0 fitting the fragment $[\text{Cu}^{\text{II}}(\text{L}^1\text{SCH}_3)\text{Cl}]^+$ (Fig. S7). The effective magnetic moment of the compound was found to be $1.71 \mu_{\text{B}}$ in methanol solution, and $1.62 \mu_{\text{B}}$ in the solid state, both in agreement with a Cu(II) center with a single unpaired electron ($S = 1/2$). The EPR spectrum of compound $[\text{Cu}^{\text{II}}(\text{L}^1\text{SCH}_3)\text{Cl}_2]$ dissolved in methanol shows a rather broad, isotropic signal with a g value of 2.11, which is characteristic of a distorted square-pyramidal geometry (Fig. S9). Apart from the intense charge-transfer transitions, the absorption spectrum of the compound $[\text{Cu}^{\text{II}}(\text{L}^1\text{SCH}_3)\text{Cl}_2]$ in the solid state shows the $d-d$ transition of the copper(II) center as a broad band with a maximum at 713 nm (Fig. S8).

The UV-vis spectrum of $[\text{Cu}_2^{\text{II}}(\text{L}^1\text{SSL}^1)\text{Cl}_4]$ dissolved in methanol shows an obvious $d-d$ transition of Cu(II) at 690 nm ($\epsilon = 1.5 \times 10^2 \text{ M}^{-1} \text{ cm}^{-1}$), in addition to an absorption band at 291 nm ($\epsilon = 3.6 \times 10^3 \text{ M}^{-1} \text{ cm}^{-1}$) likely corresponding to the $\text{Cu} \leftarrow \text{Cl}$ charge transfer transition (LMCT), and a band at 258 nm ($\epsilon = 1.0 \times 10^4 \text{ M}^{-1} \text{ cm}^{-1}$) assigned to the $\pi^* \leftarrow \pi$ transition of the pyridyl groups (Fig. S10). The ESI-MS spectrum of the dinuclear compound dissolved in methanol shows a dominant peak (m/z) at 356.1 corresponding to the fragment $\frac{1}{2}[\text{Cu}_2^{\text{II}}(\text{L}^1\text{SSL}^1)\text{Cl}_2]^{2+}$, as well as a peak at 747.0 fitting the fragment $[\text{Cu}_2^{\text{II}}(\text{L}^1\text{SSL}^1)\text{Cl}_3]^+$ (Fig. S11). The effective magnetic moment of the compound was found to be $2.27 \mu_{\text{B}}$ in dimethylsulfoxide solution, slightly lower than the expected value of two isolated $S = \frac{1}{2}$ Cu(II) ions ($\mu_{\text{eff}} = 2.83$). The EPR spectrum of $[\text{Cu}_2^{\text{II}}(\text{L}^1\text{SSL}^1)\text{Cl}_4]$ dissolved in dimethylformamide is highly similar feature to that of $[\text{Cu}^{\text{II}}(\text{L}^1\text{SCH}_3)\text{Cl}_2]$, showing a broad isotropic signal with a g value of 2.10 (Fig. S12). The absorption spectrum of the compound in the solid state shows the $d-d$ transition as a broad band with maximum absorbance at 732 nm (Fig. S13).

4. Discussion and conclusion

In this manuscript, we report the synthesis of a series of mononuclear metal compounds $[\text{M}^{\text{II}}(\text{L}^1\text{SCH}_3)\text{Cl}_2]$ ($\text{M} = \text{Co}, \text{Cu}, \text{Mn}, \text{Fe}$) containing a thioether ligand as well as the dinuclear compound $[\text{Cu}_2^{\text{II}}(\text{L}^1\text{SSL}^1)\text{Cl}_4]$ containing a disulfide ligand. The crystal structures combined with the magnetic susceptibility data confirm that the metal centers in these compounds all are in high-spin states. The coordination geometries of the metal centers in the compounds $[\text{Co}^{\text{II}}(\text{L}^1\text{SCH}_3)\text{Cl}_2]$, $[\text{Cu}^{\text{II}}(\text{L}^1\text{SCH}_3)\text{Cl}_2]$, and $[\text{Mn}^{\text{II}}(\text{L}^1\text{SCH}_3)\text{Cl}_2]$ are similar to those found in the related dinuclear compounds $[\text{Co}_2^{\text{II}}(\text{L}^1\text{SSL}^1)\text{Cl}_4]$ and $[\text{Cu}_2^{\text{II}}(\text{L}^1\text{SSL}^1)\text{Cl}_4]$. The structures of the series $[\text{M}^{\text{II}}(\text{L}^1\text{SCH}_3)\text{Cl}_2]$ show an interesting continuous trend: whereas the iron(II) center in $[\text{M}^{\text{II}}(\text{L}^1\text{SCH}_3)\text{Cl}_2]$ is in an octahedral geometry with coordination of the thioether sulfur (at $2.6972(6) \text{ \AA}$), going via the manganese(II) ($2.8325(4) \text{ \AA}$) and copper(II) ($2.9961(4) \text{ \AA}$) to cobalt(II) ($5.8887(8) \text{ \AA}$) the thioether sulfur progressively is at a larger distance from the metal center. This results in distorted square-pyramidal geometries for the Cu(II) and Mn(II) centers and a trigonal-bipyramidal geometry for the Co(II) center.

This trend is also partly visible in the structures of the dinuclear compounds $[\text{M}_2^{\text{II}}(\text{L}^1\text{SSL}^1)\text{Cl}_4]$. The structure of $[\text{Co}_2^{\text{II}}(\text{L}^1\text{SSL}^1)\text{Cl}_4]$ is relatively symmetrical: both cobalt(II) ions are in trigonal-bipyramidal

geometries with the disulfide sulfur donor atoms at non-coordinating distances. The structures of $[\text{Cu}_2^{\text{II}}(\text{L}^1\text{SSL}^1)\text{Cl}_4]$ and $[\text{Fe}_2^{\text{II}}(\text{L}^1\text{SSL}^1)\text{Cl}_4]$ are asymmetric with the two metal ions in different geometries; the M-S distances are shorter, resulting in square-pyramidal or octahedral configurations for the metal ions. These shorter M-S distances result in progressively shorter metal-metal distances: in $[\text{M}_2^{\text{II}}(\text{L}^1\text{SSL}^1)\text{Cl}_4]$ the M...M distances are $8.1617(6)$, $7.762(1) \text{ \AA}$, and $6.0567(6) \text{ \AA}$ for cobalt(II), copper(II) and iron(II), respectively. The dinuclear compounds generally show longer M-S distances than the related mononuclear compounds, indicating that the disulfide sulfur atom is slightly weaker ligand than the thioether sulfur donor.

Acknowledgements

F. Jiang acknowledges the China Scholarship Council (CSC) for a personal grant (No. 201406890012). We thank Ms. Hanan Al Habobe, Mr. Jos van Brussel and Mr. Sipeng Zheng for the ESI-MS analysis.

Appendix A. Supplementary data

CCDC 1840811, 1840819, 1840820, 1840821, 1840822 contain the supplementary crystallographic data for $[\text{Co}^{\text{II}}(\text{L}^1\text{SCH}_3)\text{Cl}_2]$, $[\text{Fe}^{\text{II}}(\text{L}^1\text{SCH}_3)\text{Cl}_2]$, $[\text{Cu}^{\text{II}}(\text{L}^1\text{SCH}_3)\text{Cl}_2]$, $[\text{Mn}^{\text{II}}(\text{L}^1\text{SCH}_3)\text{Cl}_2]$, and $[\text{Cu}_2^{\text{II}}(\text{L}^1\text{SSL}^1)\text{Cl}_4]$. These data can be obtained free of charge via www.ccdc.cam.ac.uk/data_request/cif, or by emailing data_request@ccdc.cam.ac.uk, or by contacting The Cambridge Crystallographic Data Centre, 12 Union Road, Cambridge CB2 1EZ, UK; fax: +441223 336033.

Supplementary data to this article can be found online at <https://doi.org/10.1016/j.ica.2018.10.047>.

References

- [1] M. Zhao, H.-B. Wang, L.-N. Ji, Z.-W. Mao, *Chem. Soc. Rev.* 42 (2013) 8360–8375.
- [2] I.M. Wasser, S. De Vries, P. Moëne-Loccoz, I. Schröder, K.D. Karlin, *Chem. Rev.* 102 (2002) 1201–1234.
- [3] W. Nam, *ACC Chem. Res.* 40 (2007), pp. 465–465.
- [4] C. Belle, W. Rammal, J.-L. Pierre, *J. Inorg. Biochem.* 99 (2005) 1929–1936.
- [5] B.A. MacKay, M.D. Fryzuk, *Chem. Rev.* 104 (2004) 385–402.
- [6] E.C.M. Ordning-Wenker, M. van der Plas, M.A. Siegler, S. Bonnet, F.M. Bickelhaupt, C. Fonseca Guerra, E. Bouwman, *Inorg. Chem.* 53 (2014) 8494–8504.
- [7] M. Gennari, B. Gerey, N. Hall, J. Pécaut, M.N. Collomb, M. Rouzières, R. Clérac, M. Orio, C. Duboc, *Angew. Chem. Int. Ed.* 53 (2014) 5318–5321.
- [8] A.M. Thomas, B.L. Lin, E.C. Wasinger, T.D.P. Stack, *J. Am. Chem. Soc.* 135 (2013) 18912–18919.
- [9] E.C.M. Ordning-Wenker, M. van der Plas, M.A. Siegler, C. Fonseca Guerra, E. Bouwman, *Chem. Eur. J.* 20 (2014) 16913–16921.
- [10] Y. Ueno, Y. Tachi, S. Itoh, *J. Am. Chem. Soc.* 124 (2002) 12428–12429.
- [11] S. Itoh, M. Nagagawa, S. Fukuzumi, *J. Am. Chem. Soc.* 123 (2001) 4087–4088.
- [12] S. Luo, D.F. Bruggeman, M.A. Siegler, E. Bouwman, *Inorg. Chim. Acta* 477 (2018) 24–30.
- [13] S. Luo, M.A. Siegler, E. Bouwman, *Organometallics* 37 (2017) 740–747.
- [14] G. Gezer, D.D. Jiménez, M.A. Siegler, E. Bouwman, *Dalton Trans.* 46 (2017) 7506–7514.
- [15] J.D. Franolic, W.Y. Wang, M. Millar, *J. Am. Chem. Soc.* 114 (1992) 6587–6588.
- [16] B. Horn, C. Limberg, C. Herwig, B. Braun, *Inorg. Chem.* 53 (2014) 6867–6874.
- [17] X. Liu, S.K. Ibrahim, C. Tard, C.J. Pickett, *Coord. Chem. Rev.* 249 (2005) 1641–1652.
- [18] A.R. McDonald, M.R. Bukowski, E.R. Farquhar, T.A. Jackson, K.D. Koehn, M.S. Seo, R.F. De Hont, A. Stubna, J.A. Halfen, E. Münck, *J. Am. Chem. Soc.* 132 (2010) 17118–17129.
- [19] S.A. Mirza, R.O. Day, M.J. Maroney, *Inorg. Chem.* 35 (1996) 1992–1995.
- [20] T. Ohta, T. Tachiyama, K. Yoshizawa, T. Yamabe, T. Uchida, T. Kitagawa, *Inorg. Chem.* 39 (2000) 4358–4369.
- [21] E.C.M. Ordning-Wenker, M.A. Siegler, M. Lutz, E. Bouwman, *Dalton Trans.* 44 (2015) 12196–12209.
- [22] F. Jiang, M.A. Siegler, X. Sun, L. Jiang, C. Fonseca Guerra, E. Bouwman, *Inorg. Chem.* 57 (2018) 8796–8805.
- [23] G.M. Sheldrick, *Acta Crystallogr. Sect. A* 64 (2008) 112–122.
- [24] A.W. Addison, T.N. Rao, J. Reedijk, J. van Rijn, G.C. Verschoor, *J. Chem. Soc. Dalton Trans.* (1984) 1349–1356.
- [25] A. Dutta, M. Flores, S. Roy, J.C. Schmitt, G.A. Hamilton, H.E. Hartnett, J.M. Shearer, A.K. Jones, *Inorg. Chem.* 52 (2013) 5236–5245.
- [26] G.A. Bain, J.F. Berry, *J. Chem. Educ.* 85 (2008) 532.
- [27] D. Evans, *J. Chem. Soc.* (1959) 2003–2005.
- [28] A.B.P. Lever, *Inorganic Electronic Spectroscopy*, 2nd ed., Elsevier, 1984.